Output Spectrum of a Direct Digital Synthetiser

Martin Pechanec
pechanec@yahoo.com, pechanec@iname.com

December 10, 1997

Abstract

The calculation of the output spectrum of a direct digital synthesis (DDS) sinus signal generator under the phase truncation and amplitude quantization is presented. The calculation of the phase spurious signals is similar to the approach in [1]. The closed form power spectrum expression is given and the more precise result was obtained. If no noise–dithering or noise–shaping is used, the spurious signals due to the amplitude quantization are minimal at points where the spurious signals due to the phase truncation occur, and are maximal between them. The DDS simulatoin engine was also developed to prove the validity of the calculations. The first-order phase dithering was simulated and the result is given.

1 Introduction

Direct digital synthesis has drawn a considerable attention in recent years. It outperforms conventional phase–locked loop generators (PLL) in applications where fast frequency switching and very fine frequency resolution are required. With PLL techniques it is also possible to achieve small frequency step, but circuitry complexity increases considerably with decreasing frequency step. Because PPL is generally build in analog circuitry with simple fast digital dividers, the output frequency can be very high. The modern frequency synthesizers use the PLL driven by the DDS frequency reference.

The idea of digital oscillator has been proposed by Tierney *et al.* [2]. The general DDS block diagram is in Fig. 1. A linear phase samples are generated with a sampling frequency (called driving frequency) $\omega_v = 2\pi/T_v$ are generated and converted to a sampled sinusoid. A ROM–table is usually used for phase–to–sinusoid conversion. Inherently, the maximal possible generated frequency can be $\omega_o = \omega_v/2$. Because of a necessity of a low–pass filtering, a frequency lower than 2/3 of $\omega_v/2$ is usually used as a maximum generated frequency.

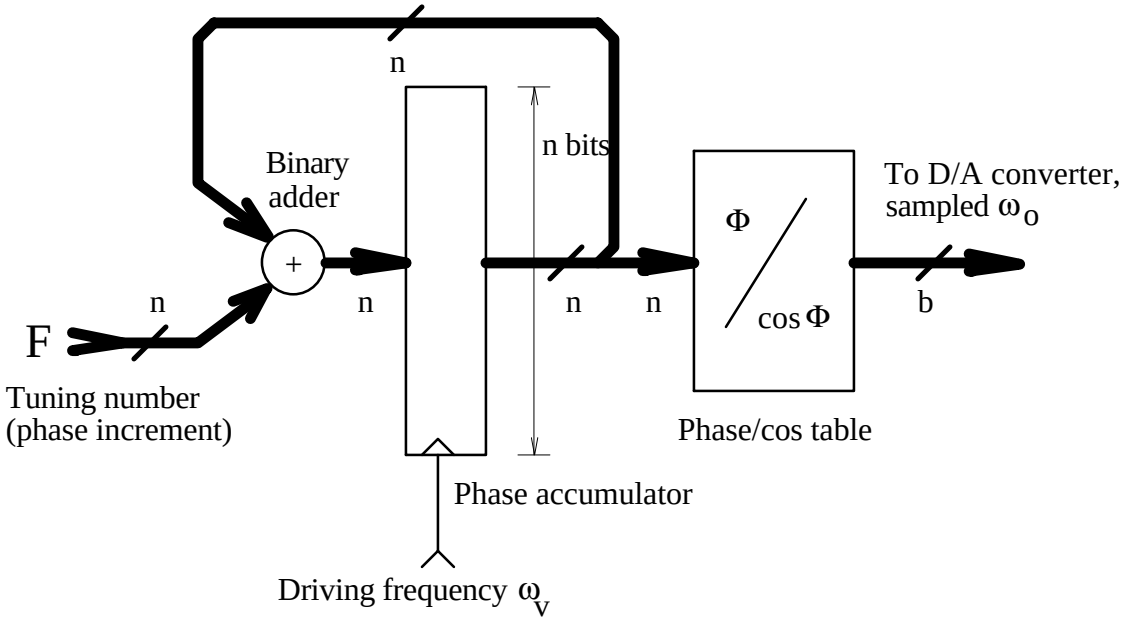

Figure 1: General DDS topology

The output frequency is derivative of the phase. By generating linearly increasing phase signal in time one can generate a constant frequency. In the DDS case, the slope of the linearly increasing phase signal is $F\frac{2\pi}{2^n}$, where F is a *tuning number* (the step increment in each clock pulse) and 2^n is the number of samples of one period of sinusoidal signal stored in a phase/cos look–up table. The minimum frequency tuning step $\Delta\omega$ (and also the minimum possible generated frequency) is

$$\Delta\omega = \frac{1}{2^n}\omega_v \tag{1}$$

and the output frequency expressed in terms of the tuning number F is

$$\omega_o = \frac{F}{2^n}\omega_v. \tag{2}$$

The output signal can be expressed as

$$s(t) = \sum_{k=-\infty}^{\infty} \cos\left(\omega_o k T_v\right) \operatorname{rect}\left(\frac{t - kT_v}{T_v}\right) \tag{3}$$

where $\operatorname{rect}(t/\tau)$ is equal 1 in the $t \in \left(-\frac{\tau}{2}, \frac{\tau}{2}\right)$ and zero otherwise. This corresponds to the widely used

sample–and–hold D/A conversion. The corresponding frequency spectrum of the signal (3) is

$$\begin{aligned} S(\omega) &= \frac{T_v}{2}\frac{\sin\omega\frac{T_v}{2}}{\omega\frac{T_v}{2}}\left[\sum_{k=-\infty}^{\infty} e^{-jkT_v(\omega-\omega_o)} + \sum_{k=-\infty}^{\infty} e^{-jkT_v(\omega+\omega_o)}\right] \\ &= \pi\frac{\sin\omega\frac{T_v}{2}}{\omega\frac{T_v}{2}}\sum_{k=-\infty}^{\infty}\left[\delta\left(\omega-(k\omega_v+\omega_o)\right)+\delta\left(\omega-(k\omega_v-\omega_o)\right)\right] \end{aligned} \tag{4}$$

where $\delta(\omega)$ is the Dirac function.

With increasing requirements on smaller frequency steps and a higher output frequency, the size of the look–up table becomes a significant problem. If, for example, the maximum required output frequency is 2.5MHz with a tuning step 1Hz, then the driving frequency f_v should be about 10MHz. The phase accumulator in Fig. 1 should have a width $n \geq \log_2 \frac{f_{omax}}{f_v}$, which is 24 bits in this case. This leads to the look–up table of the size about 16 megabytes (if 8-bit amplitude quantization is used). Utilizing the symmetry of a sinusoid, only one quarter of samples needs to be stored. Avoiding such a huge table (or complicated algorithm calculating the appropriate samples of the output signal) leads to the phase truncation.

2 Periodic signal spectum

Before the calculation of the DDS spectrum under the phase truncation is given the and the system is simulated, it is convenient to review the rectangulary sampled periodic signal spectrum. Assume a periodic signal consiting of rectangular samples

$$f(t) = \sum_{k=-\infty}^{\infty} f(nT_v)\,\mathrm{rect}\left(\frac{t-kT_v}{T_v}\right) \tag{5}$$

where $\omega_v = 2\pi/T_v$ is a sampling (angular) frequency and $T = MT_v$ is a period of the $f(t)$. Therefore $\omega_p = \frac{2\pi}{MT_v} = \frac{\omega_v}{M}$. The function $\mathrm{rect}(t/\tau)$ is defined in the text above. The Fourier transform of the $\mathrm{rect}(t/\tau)$ is

$$F\left[\mathrm{rect}\left(\frac{t}{\tau}\right)\right] = \tau\frac{\sin\omega\frac{\tau}{2}}{\omega\frac{\tau}{2}} \stackrel{\mathrm{def}}{=} R(\omega,\tau) \tag{6}$$

and

$$F\left[\mathrm{rect}\left(\frac{t-a}{\tau}\right)\right] = e^{-j\omega a}\tau\frac{\sin\omega\frac{\tau}{2}}{\omega\frac{\tau}{2}} = e^{-j\omega a}R(\omega,\tau).$$

The Fouriner tranform of the signal $f(t)$ is

$$F(\omega) = R(\omega,T_v)\sum_{k=-\infty}^{\infty} f(kT_v)e^{-j\omega kT_v}.$$

Because the function is periodic with the period $T = MT_v$, then the expression above can be written as

$$\begin{aligned} F(\omega) &= R(\omega, T_v) \sum_{n=-\infty}^{\infty} \sum_{k=0}^{M-1} f(kT_v) e^{-j\omega(nM+k)T_v} \\ &= R(\omega, T_v) \frac{2\pi}{MT_v} \sum_{n=-\infty}^{\infty} \delta\left(\omega - n\omega_p\right) \underbrace{\sum_{k=0}^{M-1} f(kT_v) e^{-j\frac{2\pi}{M}nk}}_{F(n))} \end{aligned}$$

where

$$F(n) = F(n(\mathrm{mod}\, M)) = \sum_{k=0}^{M-1} f(kT_v) e^{-j\frac{2\pi}{M}nk} = \mathrm{DFT}\left\{f(kT_v)\right\}_{k=0}^{M-1}(n)$$

which is the discrete Fourier transform of one period of the signal $f(t)$. Substituting (6), $\omega_p = \omega_v/M$, and $\tau = T_v/2$ to the equation above, we get

$$F(\omega) = \frac{\sin\omega\frac{T_v}{2}}{\omega\frac{T_v}{2}} 2\pi \sum_{k=-\infty}^{\infty} \frac{1}{M} F(n)\delta(\omega - \frac{k}{M}\omega_v). \tag{7}$$

Because the signal $f(t)$ is periodic, it can be expanded to Fourier series

$$\begin{aligned} f(t) &= \sum_{k=-\infty}^{\infty} c_k e^{j\frac{k}{M}\omega_v t} \\ c_k &= \int_{-\infty}^{\infty} f(t) e^{-j\frac{k}{M}\omega_v t} dt \end{aligned} \tag{8}$$

where c_k is the Fourier coefficient of the $k-$th harmonic. It is well know from the theory that the Fourier transform of (9) is

$$f(t) \longleftrightarrow F(\omega) = 2\pi \sum_{k=-\infty}^{\infty} c_k \delta\left(\omega - \frac{k}{M}\omega_v\right). \tag{9}$$

Comparison of (7) and (9) yields

$$c_k = \frac{\sin\omega\frac{T_v}{2}}{\omega\frac{T_v}{2}} \frac{1}{M} F(k) \tag{10}$$

for all integers k.

For practical purposes the power of each discrete harmonic component in the spectrum is of primary interest. Power of the real periodic signal of period T is defined as

$$P = \frac{1}{T}\int_0^T f^2(t) dt.$$

Because $c_{-k} = c_k^*$ for the real periodic signals the equation (9) can be written as

$$f(t) = c_0 + \sum_{k=1}^{\infty} 2|c_k| \cos\left(\frac{k}{M}\omega_v t + \arg c_k\right) \tag{11}$$

and the total power of the harmonic component at frequency $\frac{k}{M}\omega_v$ is

$$P(\frac{k}{M}\omega_v) = 2|c_k|^2 \quad \text{for} \quad k \geq 1. \tag{12}$$

Define the "finite" Dirac function as

$$d(x) = \begin{cases} 1 & : \quad x = 0 \\ 0 & : \quad x \neq 0. \end{cases} \tag{13}$$

Then the power spectrum as a set of discrete one-sided power lines of the periodic function (5) can be written as

$$P(\omega) = |\frac{f(0)}{M}|^2 d(\omega) + \sum_{k=1}^{\infty} 2 \left|\frac{\sin\frac{k}{M}\pi}{\frac{k}{M}\pi}\right|^2 \left|\frac{1}{M}F(k)\right|^2 d(\omega - \frac{k}{M}\omega_v), \tag{14}$$

which in the logarithmic domain becomes

$$P_{dB}(\omega) = 10\log P(\omega). \tag{15}$$

Because the factor $\left|\frac{\sin\frac{k}{M}\pi}{\frac{k}{M}\pi}\right|^2$ does not depend on the actual spectrum, it can be omitted when the calculation is done and then added later. All the simulations were performed and plots made without the sinc factor. The power spectrum was also adjusted by a constant to get the $0dB$ power value of fundamental beeing equal in power to the pure harmonic signal $f(t) = \cos(\omega t)$ with the amplitude equal to 1. Becasue the the power of such signal is $1/2$, the actual offset is $\Delta P_{dB} = 10\log 2$ [dB].

3 Phase truncation and a spectrum analysis

The practically used topology with the phase truncation is in Fig. 2. Instead of using the whole width of the phase accumulator, only p most significant bits are used and $q = n - p$ least significant bits are discarded, which dramatically reduces the complexity of the look-up table. The phase truncation causes spurious parasitic signals. Those signals have significant influence on the output frequency spectrum and require careful investigation.

The tuning number F can be split into two parts - the upper one of the width p bits and the lower

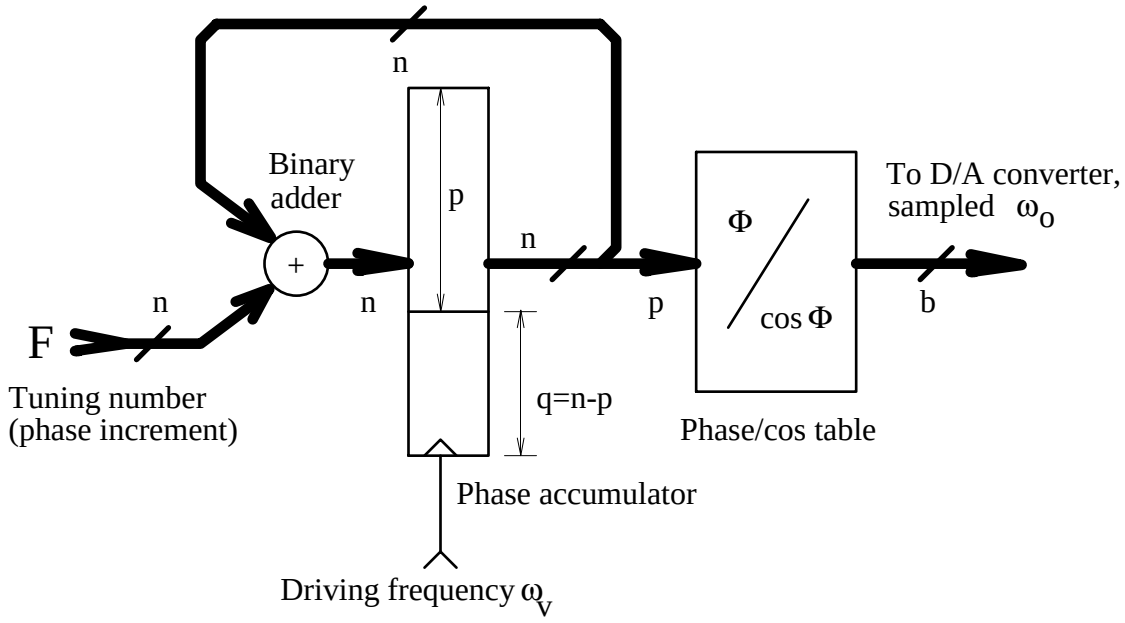

Figure 2: Phase truncated DDS

one of the width q bits. Then

$$F = F_u 2^q + F_d$$

where $F_u = 0, \ldots, 2^p - 1$ and $F_d = 0, \ldots, 2^q - 1$. If $F_d = 0$, there will be no change in the phase accumulator lower q bits and consequently no phase truncation error. Therefore, there are 2^p "clear" generated frequencies.

The case for $F_d \neq 0$ is more complicated. The maximum phase error due to the phase truncation is

$$\Delta\varphi_{max} = 2^q \frac{2\pi}{2^n} = \frac{2\pi}{2^p}.$$

The error signal is a sampled sawtooth signal having an amplitude $2\pi/2^p$. The output signal can be written in the form

$$\tilde{s}(t) = \sum_{k=-\infty}^{\infty} \cos\left(\omega_o k T_v - \Delta\varphi\left(kT_v\right)\right) \operatorname{rect}\left(\frac{t - kT_V}{T_V}\right) \tag{16}$$

where $\Delta\varphi(t)$ is the phase error. The period of this continuous phase error signal is

$$G_e = \frac{2^{n-p}}{F_d} \tag{17}$$

in "numbers" and $T_e = T_v G_e$ in time. The frequency of the phase error is $f_e = f_v \frac{1}{G_e} = f_v \frac{F_d}{2^{n-p}}$. The

continuous phase error is then

$$\Delta\varphi(t) = \frac{1}{2^p}\left[\omega_v t \frac{F_d}{2^{n-p}} \bmod 2\pi\right]. \tag{18}$$

The sampled phase error can be written as

$$\Delta\varphi\left(kT_v\right) = \frac{1}{2^p}\left[\omega_v t \frac{F_d}{2^{n-p}} \bmod 2\pi\right]. \tag{19}$$

For further analysis we have to expand the periodic phase error signal to Fourier series representation. However, analysis of (18) and (19) by Fourier series expansion requires a special approach. As mentioned in [1], based on [3], the sampled phase signal has samples at the points of discontinuities of the continuous phase error signal where Fourier series converges to the arithmetic average of limits. The situation is illustrated in Fig. 4 for $q = n - p = 3$ and $F_d = 3$. To tackle this problem, in [1] the additional "correction"

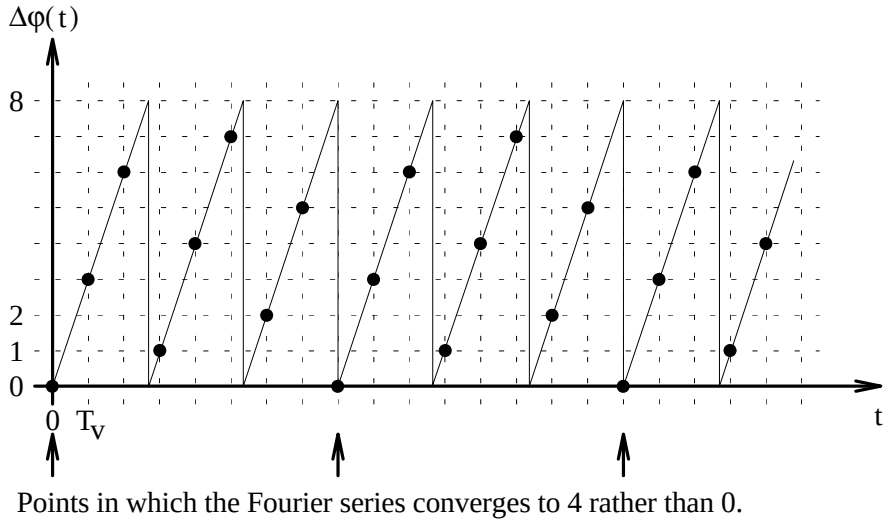

Figure 3: Period continuous and sampled phase error

additive phase signal was used to get the right expression. A different approach is presented in this paper, which does not introduce any additional artificial phase signal.

We can base our reasoning on the fact that the the phase error is known only in the discrete points. Therefore, it is up to us to interpolate those points by a continuous periodic fuction, expand it to Fourier series, and sample the Fourier series at the same points the phase error is known. We can slightly move the continuous underlying phase error in phase so that none of the phase error samples are at the points of discontinuities of the Fourier series expansion of the continuous signal. However, this slight move must not affect other points. This approach is illustrated in Fig. 4 for $q = n - p = 3$ and $F_d = 2$. The interpolating

continuous sawtooth phase error signal is shifted in time by an arbitrarily small step $\xi/2$, which causes an amplitude shift

$$c = \frac{\xi}{2}\frac{A}{P}$$

where

$$P = T_e = \frac{2^{n-p}}{F_d}T_v \tag{20}$$

is a period of the continuous sawtooth signal and

$$\boxed{A = \Delta\varphi_{max} = \frac{2\pi}{2^p}} \tag{21}$$

is the amplitude of the phase error signal. The amplitude shift is justifiable because the phase error signal will always be less than A. Just for convenience it is assumed that $\xi > 0$. The continuous unsampled

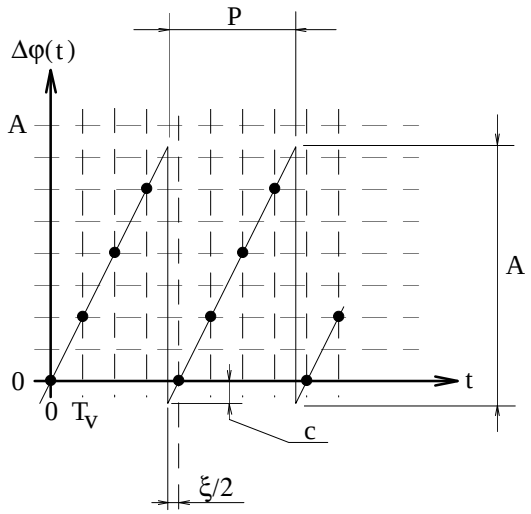

Figure 4: Phase samples and a shift

expression of the phase error signal is then

$$\Delta\varphi(t) = \frac{A}{2}\left(1 - \frac{\xi}{P}\right) - \frac{A}{\pi}\sum_{k=1}^{\infty}\frac{1}{k}\sin\left(k\frac{2\pi}{P}\left(t + \frac{\xi}{2}\right)\right), \tag{22}$$

which can be expanded to

$$\begin{aligned}\Delta\varphi(t) &= \frac{A}{2}\left(1-\frac{\xi}{P}\right)- \\ &\quad -\frac{A}{\pi}\sum_{k=1}^{\infty}\frac{1}{k}\left[\sin\left(\frac{2\pi}{P}kt\right)\cos\left(\frac{\pi\xi}{P}k\right)+\cos\left(\frac{2\pi}{P}kt\right)\sin\left(\frac{\pi\xi}{P}k\right)\right].\end{aligned} \tag{23}$$

The sampled phase error signal is then

$$\begin{aligned}\Delta\varphi(hT_v) &= \frac{A}{2}\left(1-\frac{\xi}{P}\right)- \\ &\quad -\frac{A}{\pi}\sum_{k=1}^{\infty}\frac{1}{k}\left[\sin\left(\frac{2\pi}{P}khT_v\right)\cos\left(\frac{\pi\xi}{P}k\right)+\cos\left(\frac{2\pi}{P}khT_v\right)\sin\left(\frac{\pi\xi}{P}k\right)\right].\end{aligned} \tag{24}$$

There are two periodicities in the phase error signal. First, the period of the underlying continuous phase–error signal is P (20). The second period is the exact period in samples, μ, expressed by

$$\boxed{\begin{aligned}\mu &= \frac{2^{n-p}}{\mathrm{GCD}\,(F_d, 2^{n-p})} \\ &= \frac{2^{n-p}}{\mathrm{GCD}\,(F, 2^n)} = 2^{n-p-d} = 2^{q-d}\end{aligned}} \tag{25}$$

because $\mathrm{GCD}\,(F, 2^n) = 2^d$ is always a power of 2. If $\mu \leq 1$ there are no spurious signals due to the phase truncation. The argument in (24) can be expressed as

$$\frac{2\pi}{P}khT_v = \frac{2\pi}{\frac{2^{n-p}}{F_d}T_v}khT_v = \underbrace{2\pi\frac{F_d}{2^{n-p}}}_{\alpha}kh = \alpha kh$$

where

$$\boxed{\alpha = 2\pi\frac{F_d}{2^{n-p}} = 2\pi\frac{F_d}{2^q} \widehat{=} 2\pi\frac{F}{2^q}} \tag{26}$$

The variable α can be expressed either in terms of F_d or F because it is used exclusively as a multiplicative variable in the arguments of sin and cos and the difference in value if expressed in terms of F is the integer multiple of 2π, which has no effect on the value of the sin and cos functions.

The harmonic terms in the expression (24) can be written as periodic with the period μ. Therefore, there will be two summations; the finite one (in index l) over one period and the infinite one (in index g)

over the periods

$$k = \underbrace{1, 2, \ldots, \mu - 1}_{g=1}, \underbrace{\mu, \mu + 1, \ldots, 2\mu - 1}_{g=2}, \ldots$$

where $l = 1, \ldots, \mu - 1$ and $g = 1, \ldots, \infty$. Therefore

$$k = l + (g - 1)\mu. \tag{27}$$

For further analysis it is convenient to write (24) as

$$\boxed{\Delta\varphi(hT_v) = \frac{A}{2}\left(1 - \frac{\xi}{P}\right) - \frac{A}{\pi}\left(S_1 + S_2\right)} \tag{28}$$

and analyze S_1 and S_2 separately.

3.1 Analysis of S_1

The term S_1 can be written as

$$S_1 = \sum_{k=1}^{\infty} \frac{1}{k} \sin\left(\frac{2\pi}{P} k h T_v\right) \cos\left(\frac{\pi\xi}{P} k\right) = \sum_{k=1}^{\infty} \frac{1}{k} \sin\left(\alpha k h\right) \cos\left(\frac{\alpha}{2}\frac{\xi}{T_v} k\right).$$

The same approach for simplifying S_1 as in [1] is used. Rewritting S_1 into double summation form yields

$$S_1 = \sum_{g=1}^{\infty} \sum_{l=1}^{\mu-1} \frac{1}{l + (g-1)\mu} \sin\left(\alpha h \left(l + (g-1)\,\mu\right)\right) \cos\left(\frac{\alpha}{2}\frac{\xi}{T_v} h \left(l + (g-1)\,\mu\right)\right). \tag{29}$$

If the index g is shifted by one, the equation becomes

$$S_1 = \sum_{g=1}^{\infty} \sum_{l=1}^{\mu-1} \frac{1}{l + g\mu} \sin\left(\alpha h \left(l + g\mu\right)\right) \cos\left(\frac{\alpha}{2}\frac{\xi}{T_v} h \left(l + g\mu\right)\right) + \underbrace{\sum_{l=1}^{\mu-1} \frac{1}{l} \sin\left(l\alpha h\right) \cos\left(\frac{\alpha}{2}\frac{\xi}{T_v} l h\right)}_{g=1 \text{ in } (29)}. \tag{30}$$

To get the close form expression for the infinite summation it is convenient to sum up only to $\frac{\mu}{2} - 1$ in the inner summation and rearrange the indices. Note that it is possible, because $\mu > 1$ for spurious signals to occur and it is always a power of 2. New arrangement of indices in terms of the original summation index

k is as follows

$$k = \underbrace{1,2,\ldots,\frac{\mu}{2}-1}_{\text{separate } \frac{\mu}{2}-1 \text{ terms}}, \underbrace{\frac{\mu}{2}, \underbrace{\frac{\mu}{2}+1,\ldots,\mu-1}_{\frac{\mu}{2}-1 \text{ terms...}-l \text{ part}}, \mu, \underbrace{\mu+1,\ldots,\mu+\frac{\mu}{2}-1}_{\frac{\mu}{2}-1 \text{ terms...}+l \text{ part}}}_{g=1}, \ldots$$

Expression (30) then becomes

$$\begin{aligned} S_1 &= \sum_{g=1}^{\infty}\left[\sum_{l=1}^{\frac{\mu}{2}-1}\frac{1}{l+g\mu}\sin\left(\alpha h\left(l+g\mu\right)\right)\cos\left(\frac{\alpha}{2}\frac{\xi}{T_v}h\left(l+g\mu\right)\right)+\right. \\ &\quad \left.+\sum_{l=1}^{\frac{\mu}{2}-1}\frac{1}{-l+g\mu}\sin\left(\alpha h\left(-l+g\mu\right)\right)\cos\left(\frac{\alpha}{2}\frac{\xi}{T_v}h\left(-l+g\mu\right)\right)\right]+ \\ &\quad +\sum_{l=1}^{\frac{\mu}{2}-1}\frac{1}{l}\sin\left(l\alpha h\right)\cos\left(\frac{\alpha}{2}\frac{\xi}{T_v}lh\right)+ \\ &\quad +\sum_{g=1}^{\infty}\frac{1}{g\frac{\mu}{2}}\sin\left(\alpha hg\frac{\mu}{2}\right)\cos\left(\frac{\alpha}{2}\frac{\xi}{T_v}g\frac{\mu}{2}\right). \end{aligned} \tag{31}$$

The last summation in (31)is zero, because

$$\alpha\mu = 2\pi\frac{F}{\mathrm{GCD}\left(F,2^n\right)} = K2\pi \tag{32}$$

where K is an integer. Using (32) in (31) and realizing that

$$\sin\left(\alpha h\left(g\mu\pm l\right)\right) = \underbrace{\sin\left(\alpha hg\mu\right)}_{0}\cos\left(\alpha hl\right) \pm \underbrace{\cos\left(\alpha hg\mu\right)}_{1}\sin\left(\alpha hl\right) = \pm\sin\left(\alpha hl\right)$$

we get

$$\begin{aligned} S_1 &= \sum_{l=1}^{\frac{\mu}{2}-1}\left[\frac{1}{l}\cos\left(\gamma l\right)+\right. \\ &\quad \left.+\sum_{g=1}^{\infty}\left(\frac{1}{l+g\mu}\cos\left(\gamma\left(l+g\mu\right)h\right)+\frac{1}{l-g\mu}\cos\left(\gamma\left(l-g\mu\right)h\right)\right)\right]\sin\left(\alpha hl\right) \end{aligned} \tag{33}$$

where

$$\gamma = \frac{\alpha}{2}\frac{\xi}{T_v} = \frac{F_d\pi}{2^q}\frac{\xi}{T_v}. \tag{34}$$

Equation (33) involves an expression

$$\cos\left(\gamma\left(l \pm g\mu\right)\right) = \cos\left(\gamma l\right)\cos\left(\gamma g\mu\right) \mp \sin\left(\gamma l\right)\sin\left(\gamma g\mu\right). \tag{35}$$

The choice of the time shift $\xi/2$ should simplify (35) as much as possible and must not affect any values of the sampled phase–error signal.

The maximum usable time shift ξ should be specified before we proceed. The shift must be less than the closest sampled point to the point of discontinuity ("vertical edge"). The minimum distance of the closest point from the maximum amplitude value for the phase error for a given F_d is $\frac{2\pi}{2^n}\,\mathrm{GCD}\left(F_d, 2^q\right)$ and the slope of the sawtooth signal is given by (17). The equation for the maximum possible ξ is then

$$\frac{\frac{2\pi}{2^n}\,\mathrm{GCD}\left(F_d, 2^q\right)}{\frac{\xi}{2}} = \frac{\frac{2\pi}{2^p}}{\frac{2^{n-p}}{F_d}T_v}$$

giving

$$0 < \frac{\xi}{T_v} < \frac{2\,\mathrm{GCD}\left(F_d, 2^{n-p}\right)}{f_d}. \tag{36}$$

The appropriate choice of maximum simplification of (33) is

$$\frac{\xi}{T_v} = \frac{\mathrm{GCD}\left(F_d, 2^q\right)}{f_d} = \frac{1}{\mu}\frac{2^q}{F_d}, \tag{37}$$

which is exactly one half of the upper bound of the given by (36). It follows directly from (37) and (34) that

$$\boxed{\gamma = \frac{\pi}{\mu}} \tag{38}$$

simplifying (35) to

$$\cos\left(\gamma\left(l \pm g\mu\right)\right) = (-1)^g \cos\left(\gamma l\right)$$

and the equation (33) to the form

$$S_1 = \sum_{l=1}^{\frac{\mu}{2}-1}\left[\sum_{g=1}^{\infty}\left(\frac{1}{l+g\mu} + \frac{1}{l-g\mu}\right)(-1)^g + \frac{1}{l}\right]\cos\left(\gamma l\right)\sin\left(\alpha h l\right). \tag{39}$$

For simplification of (39) the equation number 769, page 146 in [4] was used:

$$\frac{1}{\Theta}+\sum_{g=1}^{\infty}(\frac{1}{\Theta+g\pi}+\frac{1}{\Theta-g\pi})(-1)^g=\frac{1}{\Theta}+\sum_{g=1}^{\infty}\frac{2\Theta(-1)^g}{\Theta^2-g^2\pi^2}=\frac{1}{\sin\Theta}\quad\text{for}\quad\Theta\neq g\pi. \tag{40}$$

Multiplying the inner summation by $\frac{\gamma}{\gamma}$ gives $\Theta=\frac{\pi l}{\mu}$, which is never equal to any multiple of π due to the range of the index $l=1,\ldots,\frac{\mu}{2}-1$. Therefore, the simplified expression of S_1 is

$$\boxed{S_1=\frac{\pi}{\mu}\sum_{l=1}^{\frac{\mu}{2}-1}\operatorname{cotg}\left(\frac{\pi l}{\mu}\right)\sin\left(\alpha h l\right)} \tag{41}$$

3.2 Analysis of S_2

In the equations (24) and (28) the term S_2 is

$$S_2=\sum_{k=1}^{\infty}\frac{1}{k}\cos\left(\frac{2\pi}{P}khT_v\right)\sin\left(\frac{\pi\xi}{P}k\right)=\sum_{k=1}^{\infty}\frac{1}{k}\cos\left(\alpha kh\right)\sin\left(\frac{\alpha}{2}\frac{\xi}{T_v}k\right).$$

Rewriting this expression in new indices as in (31) yields

$$\begin{aligned}S_2 \;=\; & \sum_{g=1}^{\infty}\left[\sum_{l=1}^{\frac{\mu}{2}-1}\frac{1}{l+g\mu}\cos\left(\alpha h\left(l+g\mu\right)\right)\sin\left(\frac{\alpha}{2}\frac{\xi}{T_v}h\left(l+g\mu\right)\right)+\right.\\ & \left.+\sum_{l=1}^{\frac{\mu}{2}-1}\frac{1}{-l+g\mu}\cos\left(\alpha h\left(-l+g\mu\right)\right)\sin\left(\frac{\alpha}{2}\frac{\xi}{T_v}h\left(-l+g\mu\right)\right)\right]+\\ & +\sum_{l=1}^{\frac{\mu}{2}-1}\frac{1}{l}\cos\left(l\alpha h\right)\sin\left(\frac{\alpha}{2}\frac{\xi}{T_v}lh\right)+\\ & +\sum_{g=1}^{\infty}\frac{1}{g\frac{\mu}{2}}\cos\left(\alpha hg\frac{\mu}{2}\right)\sin\left(\frac{\alpha}{2}\frac{\xi}{T_v}g\frac{\mu}{2}\right).\end{aligned} \tag{42}$$

Note that the last summation in (42) is not zero as in the equation (31). Using

$$\cos\left(\alpha h\left(g\mu\pm l\right)\right)=\underbrace{\cos\left(\alpha hg\mu\right)}_{1}\cos\left(\alpha hl\right)\mp\underbrace{\sin\left(\alpha hg\mu\right)}_{0}\sin\left(\alpha hl\right)=\pm\cos\left(\alpha hl\right)$$

we get

$$\begin{aligned} S_2 &= \sum_{l=1}^{\frac{\mu}{2}-1} \left[\frac{1}{l} \sin(\gamma l) + \right. \\ &\left. + \sum_{g=1}^{\infty} \left(\frac{1}{l+g\mu} \sin(\gamma (l+g\mu) h) + \frac{1}{l-g\mu} \sin(\gamma (l-g\mu) h) \right) \right] \cos(\alpha h l) + \\ &+ \sum_{g=1}^{\infty} \frac{1}{g\frac{\mu}{2}} \sin\left(\gamma \frac{\mu}{2} g\right) \cos\left(\alpha h g \frac{\mu}{2}\right). \end{aligned} \tag{43}$$

Using equation (38) in

$$\begin{aligned} \sin(\gamma (l \pm g\mu)) &= \sin(\gamma l)\cos(\gamma g\mu) \pm \cos(\gamma l)\sin(\gamma g\mu) \\ &= \sin(\gamma l)\cos(g\pi) \\ &= (-1)^g \sin(\gamma l) \end{aligned}$$

simplifies (43) to

$$\begin{aligned} S_2 &= \sum_{l=1}^{\frac{\mu}{2}-1} \left[\sum_{g=1}^{\infty} \left(\frac{1}{l+g\mu} + \frac{1}{l-g\mu}\right)(-1)^g + \frac{1}{l} \right] \sin(\gamma l)\cos(\alpha h l) + \\ &+ \sum_{g=1}^{\infty} \frac{1}{g\frac{\mu}{2}} \sin\left(\frac{\pi}{2} g\right) \cos\left(\alpha h g \frac{\mu}{2}\right). \end{aligned} \tag{44}$$

First, we have to simplify the last term in (44). The argument of cos is an integer multiple of π determined by the value of indices g and h. Using equations number 508 and 509 in [4] on page 96

$$\begin{aligned} \sum_{k=1}^{\infty} \frac{\sin k\Theta}{k} &= \frac{1}{2}(\pi - \Theta) \quad \text{for} \quad 0 < \Theta < 2\pi \\ \sum_{k=1}^{\infty} (-1)^{k-1} \frac{\sin k\Theta}{k} &= \frac{\Theta}{2} \quad \text{for} \quad -\pi < \Theta < \pi \end{aligned}$$

gives

$$\sum_{g=1}^{\infty} \frac{1}{g\frac{\mu}{2}} \sin\left(\frac{\pi}{2} g\right) \cos\left(\alpha h g \frac{\mu}{2}\right) = \begin{cases} -\frac{\pi}{2\mu} & \text{for } h \text{ odd} \\ -\frac{\pi}{2\mu} + \frac{\pi}{\mu} & \text{for } h \text{ even} \end{cases} \tag{45}$$

Applying (45) and using the equation (40) to simplify the inner summation in (44), we get the final expression for simplified S_2 as

$$\boxed{S_2 = \frac{\pi}{\mu}\left[\sum_{l=1}^{\frac{\mu}{2}-1}\cos(\alpha h l) + \frac{1}{2}(-1)^h\right]} \tag{46}$$

3.3 Spectrum calculation

Combining (41), (46), (24), and $\xi/P = 1/\mu$, we get the expression for the sampled error phase signal in the simplified form

$$\Delta\varphi(hT_v) = \frac{A}{2}\left(1 - \frac{1}{\mu}\left(1 + (-1)^h\right)\right) - \frac{A}{\mu}\sum_{l=1}^{\frac{\mu}{2}-1}\left[\operatorname{cotg}\left(\frac{\pi l}{\mu}\right)\sin(\alpha h l) + \cos(\alpha h l)\right]. \tag{47}$$

The term in square brackets has the general form of $c = a\sin b + \cos b$ where $a = \operatorname{cotg} b$ and

$$b = \frac{\pi l}{\mu} < \frac{\pi}{2}.$$

It can be easily shown that

$$c = \sqrt{1+a^2}\cos(\beta + \operatorname{arctg} a).$$

An analytical expression for $\operatorname{arctg} a = arctg(\operatorname{cotg} b)$ should be found. It is obvious that for $b < \pi/2$ it becomes $\operatorname{arctg} a = \pi/2 - b$ and therefore

$$c = \frac{1}{\sin b}\sin(\beta + b).$$

Using the expression above in (47) we get

$$\Delta\varphi(hT_v) = \frac{A}{2}\left(1 - \frac{1}{\mu}\left(1 + (-1)^h\right)\right) - \sum_{l=1}^{\frac{\mu}{2}-1}\frac{A}{\mu\sin\frac{\pi l}{\mu}}\sin\left(\alpha h l + \frac{\pi l}{\mu}\right). \tag{48}$$

The final expression for the spectrum of (16) is

$$\boxed{\begin{aligned}\tilde{S}(\omega) &= \frac{T_v}{2}\frac{\sin\omega\frac{T_v}{2}}{\omega\frac{T_v}{2}}S_h(\omega)\\ S_h(\omega) &= \sum_{h=-\infty}^{\infty}2\cos\left(\gamma_h + \sum_{l=1}^{\frac{\mu}{2}-1}\beta_l\sin\alpha_{hl}\right)e^{-j\omega h T_v}\end{aligned}} \tag{49}$$

where

$$\gamma_h = \omega_o h T_v - \frac{A}{2}\left(1 - \frac{1}{\mu}\left(1 + (-1)^h\right)\right), \tag{50}$$

$$\beta_l = \frac{A}{\mu \sin\frac{\pi l}{\mu}} = \frac{2\pi}{2^p \mu \sin\frac{\pi l}{\mu}} < \frac{\pi}{2^p}, \tag{51}$$

$$\alpha_{hl} = \alpha h l + \frac{\pi l}{\mu} = \omega_v \frac{F_d}{2^q} l h T_v + \frac{\pi l}{\mu}. \tag{52}$$

Let us investigate the $S_h(\omega)$ term. The first argument in the summations the cos function with a time varying phase. This involves Bessel functions and it cannot be easily simplified. The cos summation can be written as

$$\begin{aligned} 2\cos(\gamma_h + \sum_{l=1}^{\frac{\mu}{2}-1} \beta_l \sin\alpha_{hl}) &= e^{j\gamma_h} e^{j\sum_{l=1}^{\frac{\mu}{2}-1}\beta_l \sin\alpha_{hl}} + e^{-j\gamma_h} e^{-j\sum_{l=1}^{\frac{\mu}{2}-1}\beta_l \sin\alpha_{hl}} \\ &\approx e^{j\gamma_h}(1 + j\sum_{l=1}^{\frac{\mu}{2}-1}\beta_l \sin\alpha_{hl}) + e^{-j\gamma_h}(1 - j\sum_{l=1}^{\frac{\mu}{2}-1}\beta_l \sin\alpha_{hl}) \end{aligned} \tag{53}$$

where the first order approximation of the exponential functions was used. It is justifiable only if

$$\sum_{l=1}^{\frac{\mu}{2}-1} \beta_l \sin\alpha_{hl} \ll 1.$$

In practice p is large, in most cases $p > 10$, then (51) shows clearly that $\beta_l \ll 1$ and also $A \ll 1$. Therefore, the approximation (53) is justified. Combining (53) with (49) we get

$$\begin{aligned} S_h(\omega) = \frac{\pi}{T_v}\Bigg\{ & \sum_{k=-\infty}^{\infty}\left[c_k\delta(\omega_o - \frac{\omega_v}{2}k - \omega) + c_k^*\delta(\omega_o - \frac{\omega_v}{2}k + \omega)\right] + \\ + & \sum_{l=1}^{\frac{\mu}{2}-1}\frac{\beta_l}{2}\Bigg[\sum_{k=-\infty}^{\infty}\Big(c_k e^{j\frac{\pi l}{\mu}}\delta(\omega_o + \omega_v d_k - \omega) - \\ & -c_k e^{-j\frac{\pi l}{\mu}}\delta(\omega_o - \omega_v d_k - \omega) - \\ & -c_k^* e^{j\frac{\pi l}{\mu}}\delta(\omega_o - \omega_v d_k + \omega) + \\ & +c_k^* e^{-j\frac{\pi l}{\mu}}\delta(\omega_o + \omega_v d_k + \omega)\Big)\Bigg]\Bigg\} \end{aligned} \tag{54}$$

where

$$\boxed{d_k = \frac{F_d}{2^q} l - \frac{k}{2}} \tag{55}$$

and

$$c_k = e^{-j\frac{A}{2}}(e^{j\frac{A}{\mu}} + e^{jk\pi}) = e^{-j\frac{A}{2}}(e^{j\frac{A}{\mu}} + (-1)^k).$$

The expression (54) clearly distinguishes between desired output signals and trains of parasitic impulses. There are 4 trains of spurious signals in the spectrum. The first one starts at the frequency ω_0 and the second one at the frequency $-\omega_0$. Since p is assumed to be reasonable large (greater than 10) to make $A \ll 1$, the exponentials in c_k can be again approximated by the first order terms yielding

$$c_k = 1 + (-1)^k - j\frac{A}{2}(1 + (-1)^k) + j\frac{A}{\mu}$$

and therefore

$$\boxed{\begin{aligned} c_{ko} &= j\frac{A}{\mu} \quad \text{for } k \text{ odd} \\ c_{ke} &= 2 - jA(1 - \frac{1}{\mu}) \quad \text{for } k \text{ even} \end{aligned}} \tag{56}$$

There are two other trains of impulses in the spectrum. These are the trains of fundamentals separated by the driving frequency ω_v and causing spurious signals at frequencies $\pm\omega_0 \pm k\frac{\omega_v}{2}$. To get the proper closed form expression for the spectal lines we have to investigate whether some of the Dirac impulses in (54) overlap each other.

The equation (54) is divied into odd and even parts according to the value of the summation index k. Define a value

$$Q = \frac{F_d}{\mathrm{GCD}\,(F_d, 2^q)} \quad \ldots \text{ odd number} \tag{57}$$

which is always odd positive integer and which becomes handy later.

Let us illustrate the procedure for even k. First, we have to make sure there are no overlaps from the positive and negative parts of the same train. Let us assume there is an overlap. In such a case there must exist indices l_1, l_2, k_1, k_2 such that

$$\begin{aligned} \omega_v\left(\frac{F_d}{2^q}l_1 - k_1\right) &= -\omega_v\left(\frac{F_d}{2^q}l_2 - k_2\right) \\ \frac{F_d}{2^q}(l_1 + l_2) &= k_1 + k_2. \end{aligned}$$

Using equations (57) and (25) and realizing that $\mu = 2^{q-d} > 1$ for spurious signals to happen, we get

$$\frac{Q}{\mu}(l_1 + l_2) = k_1 + k_2.$$

Becasue Q is odd and μ is even, for the equation above to be true for integer indices, the eqaulity

$$l_1 + l_2 \stackrel{!}{=} \mu$$

should be satisfied. This is not possible, because both l_1 and l_2 ranges from 1 to $\frac{\mu}{2} - 1$. Therefore, there is no overlap from the same impulse train.

There are 8 possible cross–train combinations of possible pulse train overlaps. Let us illustrate the procedure for the first and fourth (the same for second and third) pulse trains in the square brackets in the equation (54). For pulse trains to overlap, the equation

$$\omega_0 + \omega_v \left(\frac{F_d}{2^q} l_1 - k_1 \right) = -\omega_0 - \omega_v \left(\frac{F_d}{2^q} l_2 - k_2 \right)$$

should be satisfied. Expressing the fundamental output frequency as

$$\omega_0 = \frac{F}{2^n} \omega_v = \frac{F_u 2^q + F_d}{2^q 2^p} = \frac{F_u \mu + Q}{\mu 2^p}$$

yields

$$F_u \mu + Q = -Q 2^{p-1} (l_1 + l_2) - \mu 2^{p-1} (k_1 + k_2). \tag{58}$$

It can be easily seen that the left side of the equation (58) is always an odd integer and the right side is always an even integer for $p > 1$. As mentioned above, we assume $p > 10$, so the pulse trains mentioned above do not overlap.

The same procedure must take place for the rest of the cross–train combinations for even k. It can be shown that for even k there are no pulse overlaps at all. For odd k (it means that both k_1 and k_2 are odd), the same analysis reveals no overlap as in the previous case, where both k_1 and k_2 were even.

Further analysis, done by the same procedure as above, shows that the only overlaps exist between pulse trains where one train has k odd and the other one k even. When all the possible combination are

taken care of, the expression (54) becomes

$$\begin{aligned} S_h(\omega) &= \frac{\pi}{T_v}\left\{\sum_{k=-\infty}^{\infty}\left[c_k\delta(\omega_o-\frac{\omega_v}{2}k-\omega)+c_k^*\delta(\omega_o-\frac{\omega_v}{2}k+\omega)\right]+\right. \\ &+ \frac{A}{2\mu}\sum_{l=1}^{\frac{\mu}{2}-1}\sum_{k=-\infty}^{\infty}\Big[g_{l-}e^{j\frac{\pi l}{\mu}}\delta(\omega_o+\omega_v d_k-\omega)- \\ &\quad -g_{l+}e^{-j\frac{\pi l}{\mu}}\delta(\omega_o-\omega_v d_k-\omega)- \\ &\quad -g_{l+}^*e^{j\frac{\pi l}{\mu}}\delta(\omega_o-\omega_v d_k+\omega)+ \\ &\quad \left.+g_{l-}^*e^{-j\frac{\pi l}{\mu}}\delta(\omega_o+\omega_v d_k+\omega)\Big]\right\} \end{aligned} \tag{59}$$

where

$$g_{l\pm}=\underbrace{\frac{2}{\sin\frac{\pi l}{\mu}}\pm\frac{A}{\mu\cos\frac{\pi l}{\mu}}}_{\tilde{g}_{l\pm}}-j\frac{A\left(1-\frac{1}{\mu}\right)}{\sin\frac{\pi l}{\mu}}. \tag{60}$$

The last two terms in $g_{l\pm}$ are small in comparison with the first one. The imaginary part can be neglected because it is orthogonal to the large real part and its contribution to the absolute value of $g_{l\pm}$, and therefore to the output power spectrum, is negligible.

However, the second real term cannot be neglected. It causes some interesting asymmetry in the resulting spectrum. The influence of the second real term is around $1dB$ in the output power spectrum. In the widely cited analysis given in [1] this term was neglected and the resulting $1dB$ error in the predicted spectrum was considered to be caused by truncation and rounding of computer arithmetic. Also, the "DC" component in phase was neglected in [1], which is not justifiable, and lead to inclusion of a mysterious factor of 2 to correct the that.

To obtain a final expression for $S_h(\omega)$ we have to look back to the c_k coefficients specified by (56). Because $p > 10$ and therefore $A \ll 1$, the imaginary part of e_{ke} in (56) can be neglected, so $c_{ke} = 2$. The final closed form expression of the DDS spectrum $S_h(\omega)$, where all terms are unique (non of them overlap

any other one), is

$$
\begin{aligned}
S_h(\omega) &= \frac{2\pi}{T_v}\sum_{k=-\infty}^{\infty}\Bigg[\delta(\omega_o-\omega_v k-\omega)+\delta(\omega_o-\omega_v k+\omega)+ && (61)\\
&+ j\frac{A}{2\mu}\delta(\omega_o-\omega_v k-\frac{\omega_v}{2}-\omega)-j\frac{A}{2\mu}\delta(\omega_o-\omega_v k-\frac{\omega_v}{2}+\omega)+\\
&+ \frac{A}{4\mu}\sum_{l=1}^{\frac{\mu}{2}-1}\Bigg[\tilde{g}_{l-}e^{j\frac{\pi l}{\mu}}\delta(\omega_o+\omega_v d_k-\omega)- && (62)\\
&\quad -\tilde{g}_{l+}e^{-j\frac{\pi l}{\mu}}\delta(\omega_o-\omega_v d_k-\omega)- && (63)\\
&\quad -\tilde{g}^*_{l+}e^{j\frac{\pi l}{\mu}}\delta(\omega_o-\omega_v d_k+\omega)+ && (64)\\
&\quad +\tilde{g}^*_{l-}e^{-j\frac{\pi l}{\mu}}\delta(\omega_o+\omega_v d_k+\omega)\Bigg]\Bigg] && (65)
\end{aligned}
$$

where

$$\boxed{\tilde{g}_{l\pm}=\frac{2}{\sin\frac{\pi l}{\mu}}\pm\frac{A}{\mu\cos\frac{\pi l}{\mu}}} \qquad (66)$$

If $\mu=2$ then the last summation over the summation index l in (62) is equal to zero. The situation of pulse trains is schematically shown in Fig. 5, where the pulse trains 1+,2−,3+, and 4− corresponds to the final spectrum expression parts (63),(64),(65), and (65), respectively.

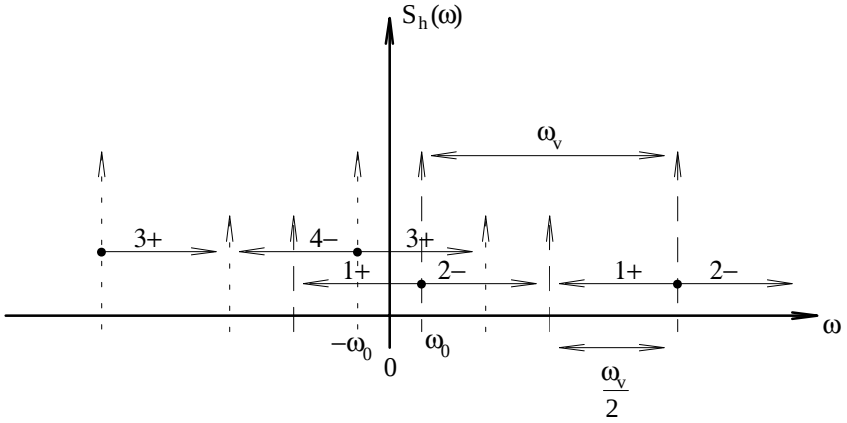

Figure 5: Discrete spectral line trains

It should be noted that the frequency separation between spurs in the same pulse train is

$$\Delta\omega_{spur}=\frac{\omega_v}{\mu}.$$

Equations (62) and (66) reveal an interesting "asymmetry" in the spectrum between the plus and minus pulse trains power levels. As mentioned above, the difference is about 1dB and was not investigated before. It should be also noted that for the actual spectrum the expression (62) should be used in (49). That step is obvious and was omitted here.

The obvious question is what the worst case spur level in a given DDS generator can be. From (62) it is obvious that if the amplitude of the desired frequency is assumed to be one, the spurious signals will have (relative) amplitude ζ from the set

$$\boxed{\zeta(\mu,l) \in \left\{ \frac{A}{2\mu}, \frac{A}{4\mu}\tilde{g}_{l\pm} \right\}_{l=1}^{\frac{\mu}{2}-1}} \tag{67}$$

at their respective frequencies, where the first term in (67) does not depend on l. To get the actual power level in [dB] we can calculate

$$\zeta_{dB}(\mu,l) = 20\log\zeta(\mu,l)\,. \tag{68}$$

Both expressions for $\zeta(\mu,l)$ do not take into account the $\frac{\sin\omega\frac{T_v}{2}}{\omega\frac{T_v}{2}}$ weighting term in (49).

Realizing that $\mu = 2,4,8,\ldots,2^q$ and inspecting the term $\tilde{g}_{l\pm}$, we can easily observe that the maximum spur has amplitude

$$\zeta_{max} = \begin{cases} \dfrac{A}{4} & \text{for} \quad \mu = 2 \\ \dfrac{A}{4\mu}\tilde{g}_{1+} & \text{for} \quad \mu > 2 \end{cases} \tag{69}$$

It implies that the maximum spur in the phase truncated DDS will have the amplitude (with respect to the amplitude of f_0) expressed by

$$\boxed{\zeta_{MAX} = \frac{A}{4} \text{ for } \mu = 2 \;\Rightarrow F_d = 2^{q-1}} \tag{70}$$

The spectral situation for both $\mu = 2$ and $\mu = 4$, without the amplitude quantization, is shown in figures 6 and 7, respectively.

4 Amplitude quantization and a spectrum analysis

All papers published so far dealt only with phase truncation error or amplitude quantization error, but not both. To deal with both of them, we first need to calculate the influence of an amplitude quantization of the samples of the output signal on the output spectrum.

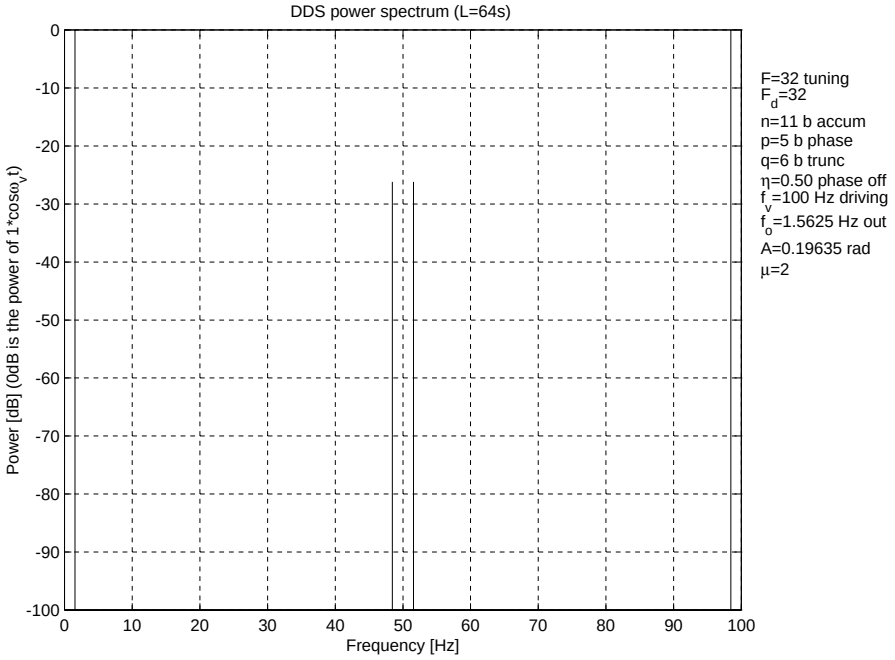

Figure 6: Output spectrum for $\mu = 2$.

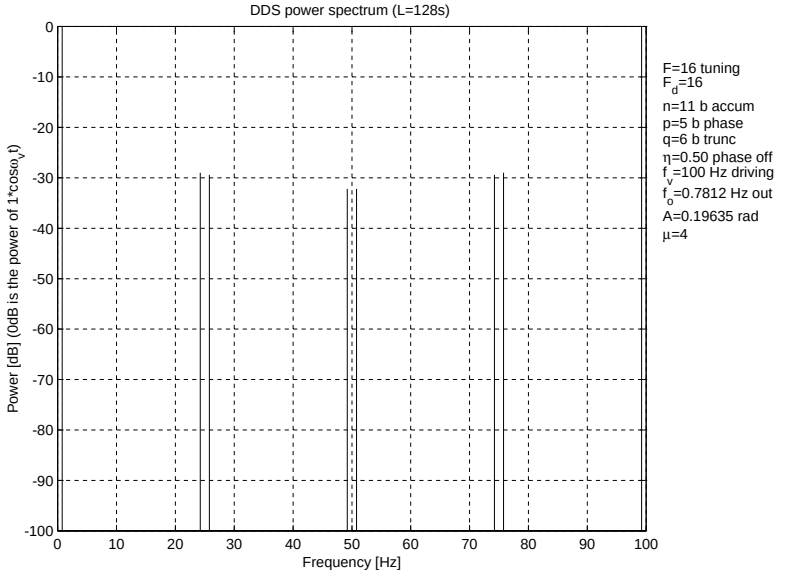

Figure 7: Output spectrum for $\mu = 4.6$.

4.1 Amplitude sampling

As mentioned above, 2^n samples needs to be stored or generated. To simplify the task, the 4–quadrant symmetry of a sinusoid is utilized in practice. To use this symmetry, samples must be stored or generated such as $\phi(k) = \frac{2\pi}{2^n}(k + \frac{1}{2})$ for $k = 0, 1, \ldots, 2^n - 1$. The phase step is $\Delta\varphi_e = \frac{2\pi}{2^n}$. The situation of the "symmetrical" sampling for $n = 4$ is in Fig. 8, where bit values for each sample are the phase values, not the amplitude values. The two most significant bits indicate the quadrant the sample is in and the rest of

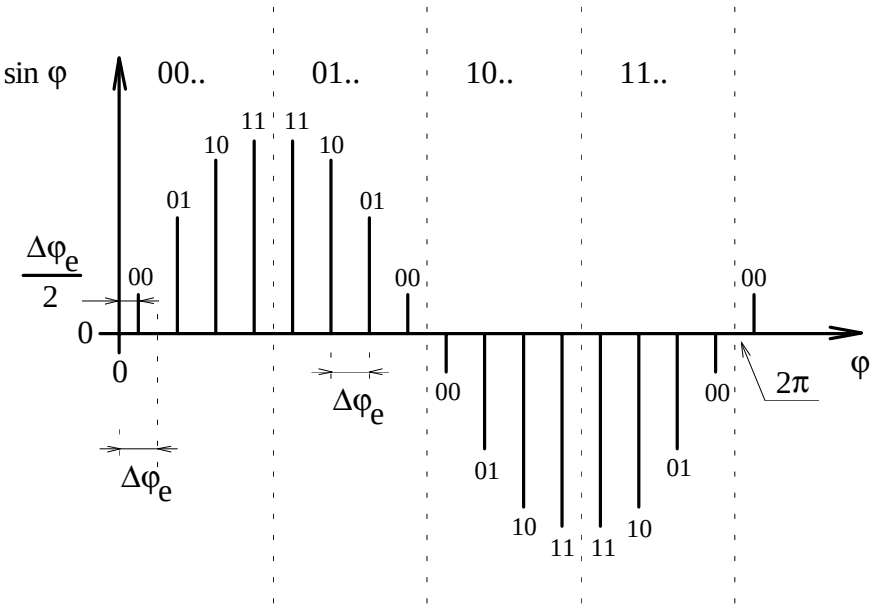

Figure 8: One period of symmetrically sampled sin function.

the bits indicate the phase inside the quadrant.

The values of the output function must be quantized. The DDS system used D/A convertor at its output to convert the digital samples to analog value. Most of the D/A converters use an integer positive arithmetic and neither 1's, nor 2's complement, the best number system for sampled amplitude is a shifted zero system. It is very convenient to center the quantization levels around zero, i.e. zero is a boundary between two adjacent quantization levels, not the center of a quantization level. The situation for $b = 3$ quantization bits is shown in Fig. (9), where solid horizontal lines denote the boundaries between two quantization levels, and horizontal dotted lines denote the centers of each quantization level. Using the discussion above we can come up with a circuit, which would realize the mapping of the one stored quadrant to the remaining three quadrants. The circuit is in Fig. 10.

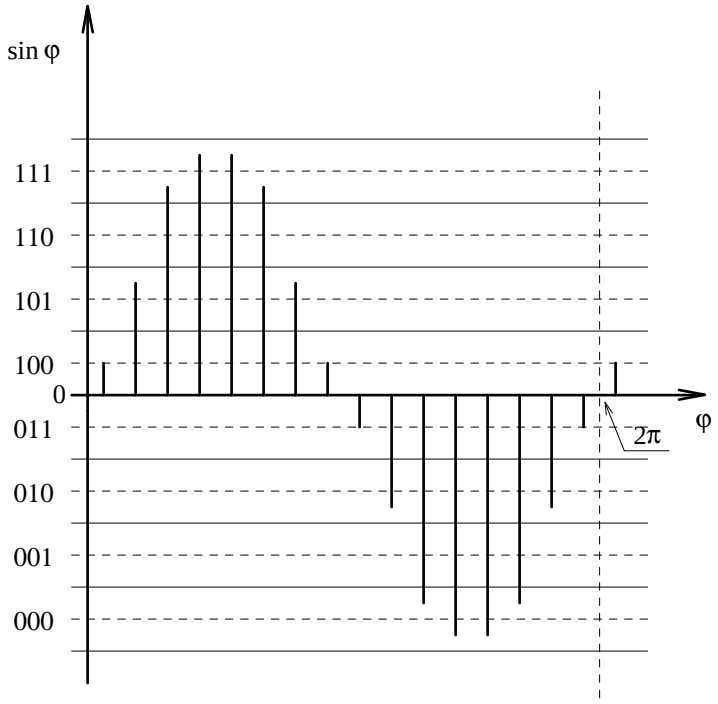

Figure 9: Quantization levels for =3 bits.

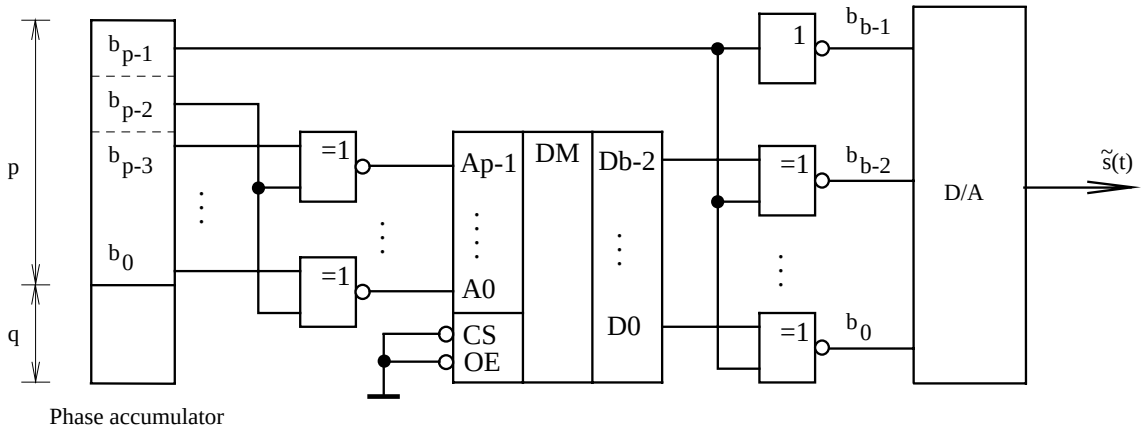

Figure 10: First sampled qadrant mapping circuit.

4.2 Spectrum calculation

The goal is to calculate the spurious signals levels caused by the amplitude quantization without the phase truncation. In that case the output signal can be expressed as

$$\hat{s}(t) = \sum_{k=-\infty}^{\infty} (cos(\omega_o k T_v) + \varepsilon_\varphi(k\Delta\varphi)) \text{ rect}\left(\frac{t - kT_v}{T_v}\right) \tag{71}$$

where $\Delta\varphi = \omega_o T_v$. The signal is periodic with a period $T_e = mT_v$, where m is an integer (to be determined). It is obvious, that the error term in (71) has an additive character and the output spectrum will be a sum of the ideal spectrum (4) and the error spectrum

$$E(\omega) = \sum_{k=-\infty}^{\infty} \varepsilon_\varphi(k\Delta\varphi) F\left[\mathrm{rect}\left(\frac{t-kT_v}{T_v}\right)\right].$$

Since the error is periodic with the period m, $E(\omega)$ can be expressed as

$$E(\omega) = \frac{2\pi}{m} \sum_{l=-\infty}^{\infty} \left[\frac{\sin\frac{\pi l}{m}}{\frac{\pi l}{m}} \delta(\omega - \frac{l}{m}\omega_v) \sum_{k=0}^{m-1} \varepsilon_\varphi(kF\Delta\varphi_e) e^{-j\frac{2\pi}{m}kl}\right]. \tag{72}$$

The error spectrum consists of discrete spurious signals separated by ω_v/m.

The error signal period m satisfies an equation $m\Delta\varphi = 2\pi r$, where r is an integer. It implies that

$$\boxed{m = \frac{2^n}{\mathrm{GCD}(F, 2^n)} = 2^{n-d}} \tag{73}$$

The second summation in (72) is clearly a discrete Fourier transform of the error signal. Because the quantization error is symmetrical and periodic with a power of 2, it has an important property

$$\varepsilon_\varphi(k - \frac{m}{2}) = -\varepsilon_\varphi(k).$$

Such signals doe not have even harmonic components. The output spectrum can be written as

$$\hat{S}(\omega) = S(\omega) + E(\omega) = \pi \frac{\sin\frac{\pi\omega}{\omega_v}}{\frac{\pi\omega}{\omega_v}} \frac{2}{m} \sum_{l=-\infty}^{\infty} \left[\delta(\omega - \frac{l}{m}\omega_v) \sum_{k=0}^{m-1} \hat{s}(kF\Delta\varphi_e) e^{-j\frac{2\pi}{m}kl}\right] \tag{74}$$

where

$$\hat{s}(k\Delta\varphi) = \cos(k\Delta\varphi) + \varepsilon_\varphi(k\Delta\varphi) \tag{75}$$

are the actual samples stored in the look–up table.

5 Phase truncation and amplitude quantization

Both phase truncation and amplitude quantization are now considered. No attention has been given to the *both* phenomena in the literature so far. Combining (16) and (71), a complete expression for the DDS output

is

$$\begin{aligned} s_b(t) &= \sum_{k=-\infty}^{\infty} (\cos(\omega_o kT_v - \Delta\varphi(kT_v)) + \varepsilon_\varphi(\omega_o kT_v - \Delta\varphi(kT_v))) \operatorname{rect}\left(\frac{t-kT_v}{T_v}\right) \\ &= \tilde{s}(t) + \underbrace{\sum_{k=-\infty}^{\infty} \varepsilon_\varphi(\omega_o kT_v - \Delta\varphi(kT_v)) \operatorname{rect}\left(\frac{t-kT_v}{T_v}\right)}_{e_{pm}(t)}, \end{aligned} \tag{76}$$

the spectrum of which is a sum of the phase truncated spectrum (49) and the spectrum of a phase–modulated quantization error signal $e_{pm}(t)$, therefore

$$S_b(\omega) = \tilde{S}(\omega) + E_{pm}(\omega).$$

Because $e_{pm}(t)$ is periodic with the same period m as in the quantization–only case, the expression of the spectrum $E_{pm}(\omega)$ will be the same as (72) (the only difference is the argument of the ε) and the $\varepsilon_\varphi(t)$ will have the same symmetry property as in the previous case.

The power spectrum can be determined by calculating the DFT

$$U(l) = \sum_{k=1}^{m-1} \varepsilon_\varphi(k\Delta\varphi_e F - \Delta\varphi(kT_v)) e^{-j\frac{2\pi}{m}kl} = \sum_{k=1}^{m-1} f(k) e^{-j\frac{2\pi}{m}kl}.$$

The sequence $f(k)$ is periodic with a period m and consists of 2^p segments, each of length μ. The values of $f(k)$ in each segment are the same. It is convenient to define a new sequence $f_\mu(k) = f(\mu k)$ for $k = 0, \ldots, 2^p - 1$, which has also the symmetry property $f_\mu(k - 2^{p-1}) = f_\mu(k)$. Therefore

$$U(l) = \frac{\sin l\pi\frac{\mu}{m}}{\sin\frac{l\pi}{m}} e^{-j\frac{l\pi}{m}(m-1)} \sum_{k=1}^{\frac{m}{\mu}-1} f_\mu(k) e^{-jkl\frac{2\pi}{m}}. \tag{77}$$

for $l = 0, \ldots, m-1$. Because of the symmetry, $U(l) = 0$ for l even. Let us denote DFT of the sequence $f_\mu(k)$ as $F_\mu(k)$. The expression (77) can be written as

$$U(l) = \frac{\sin l\pi\frac{1}{2^p}}{\sin\frac{l\pi}{m}} e^{j\frac{l\pi}{\mu}} \frac{1}{2^p} \sum_{k=1}^{2^p-1} F_\mu(k) \frac{\sin\frac{l\pi}{\mu}}{\sin\frac{\pi}{2^p}(\frac{l}{\mu} - k)} \tag{78}$$

where terms $e^{-jl\pi/2^p}$ were approximated by 1, because usually $2^p >> 1$. Comparing (78), (72), and (62) we can see, that the spurious signals caused by the phase–truncation (for no amplitude–quantization) lie at the points where $l = n\mu \pm 1$ for $n = 1, \ldots, 2^p - 1$. The weighting factor $(\sin l\pi\frac{1}{2^p})/(\sin\frac{l\pi}{m})$ is minimal at

those points. It implies that the amplitude–quantization error spectrum with the phase–truncation will have almost no influence at the power spectrum of the phase–truncation error alone. The amplitude–quantization error spectrum will reach its maximum in between the spurious levels caused by the phase–truncation. This fact is show in figures 11 to 13, where the power spectrum in Fig. 11 equals the spectrum obtained by overlapping the spectra in figures 12 and 13.

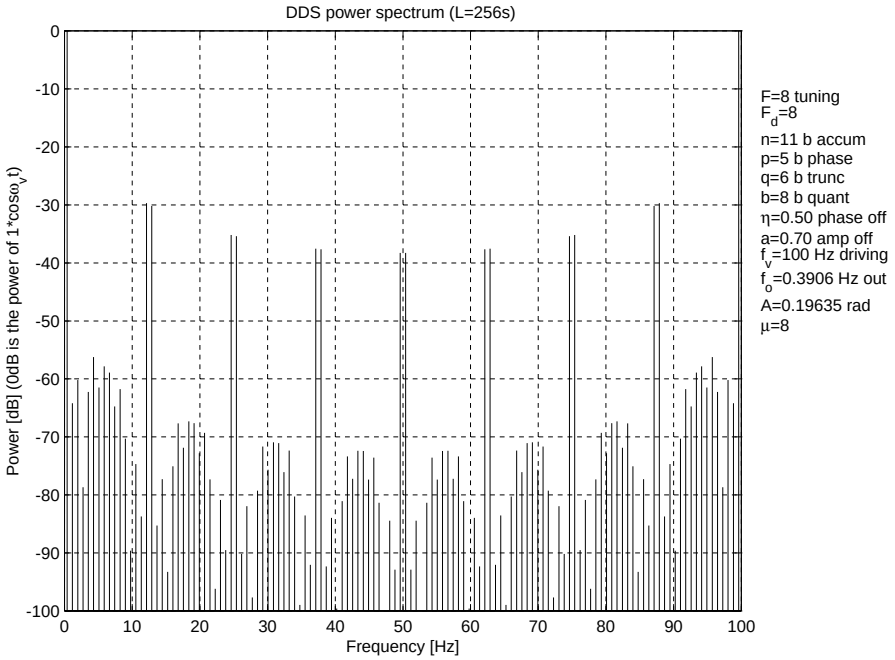

Figure 11: Complete output spectrum with both phase truncation and amplitude quantization.

As mentioned in [5], it is necessary to calculate only n power spectra for $F = 2^k$, where $k = 0, \ldots, n-1$. An output spectrum for any general F will just be permutated one of those.

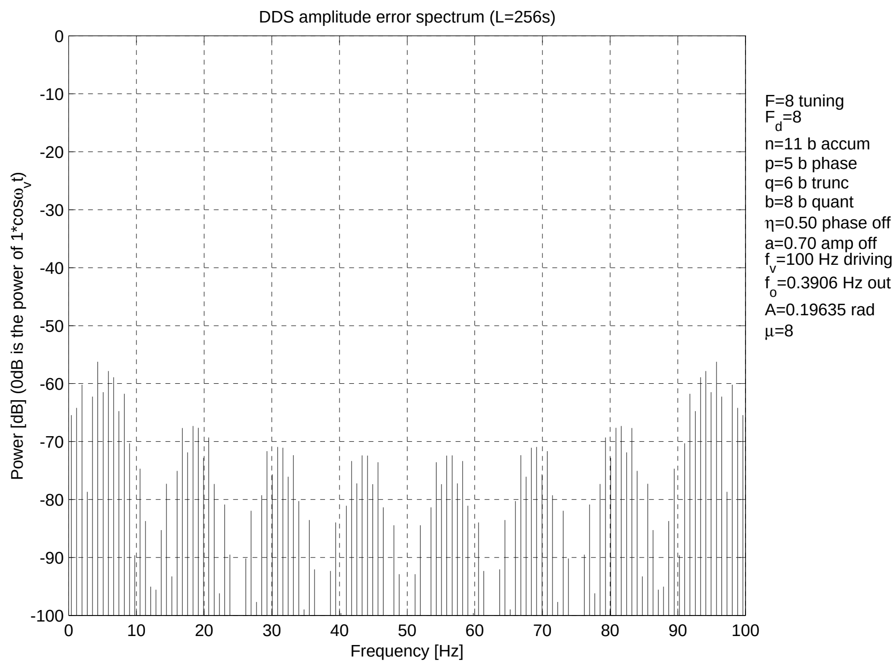

Figure [illegible] present.

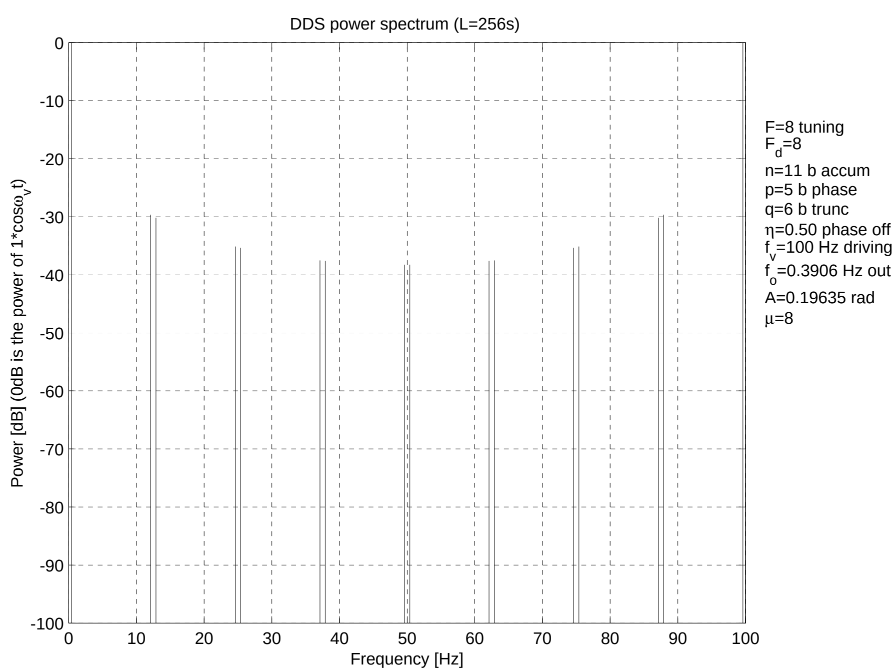

Figure 13: Output spectrum for phase truncation only.

6 Simulation

One of the primary goal of the project was to develop a universal environment in MATLAB for simulating the performance of any DDS synthetiser. New MATLAB graphic user interface (GUI) was used to interface

with a user. Also, there is a complete set of simulation parameters included in each plot. The GUI is shown in Fig. 14.

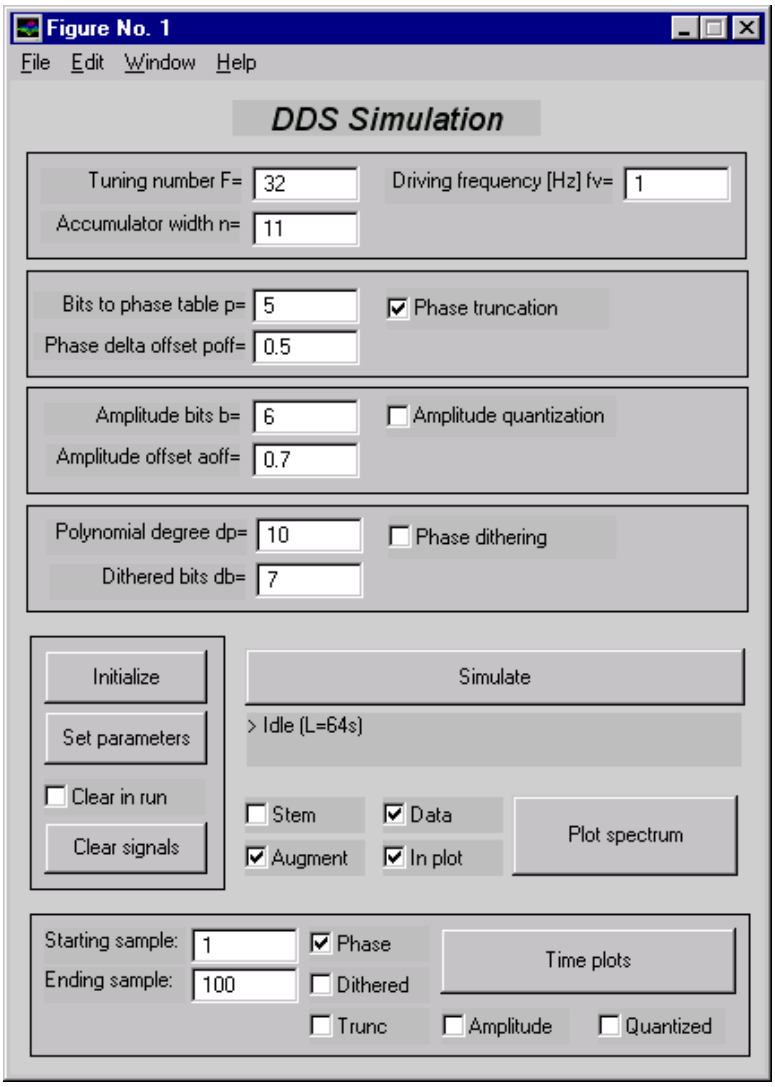

Figure 14: MATLAB simulation user interface.

6.1 Phase dithering

According to the (69) and as shown in Fig. 11, the spurious signals caused by the phase truncation can be very high. To lower them, several techniques were proposed [1, 6, 7, 8, 9, 10].

The basic idea proposed in [1] is to keep μ at its maximum, which is $\mu_{max} = 2^q$. That value is achieved if the tuning number F is odd. Therefore, by keeping the F odd we can improve the spectral performace

just about $3dB$. In the project the primary simulation effort was focused on the idea of phase dithering presented in [8, 10].

The spur signals are located at a finite number of discrete frequencies. The idea behind the dithering is the same as behind the spread spectrum systems. By adding pseudorandom noise to the deterministic periodic signal, the power of discrete components is lowered and their spectrum is spread over the wide range of frequencies. The price we pay for doing that is the rise of a noise floor.

The first–order phase dithering architecture proposed in [10] is in Fig. 15. A pseudorandom $M-$

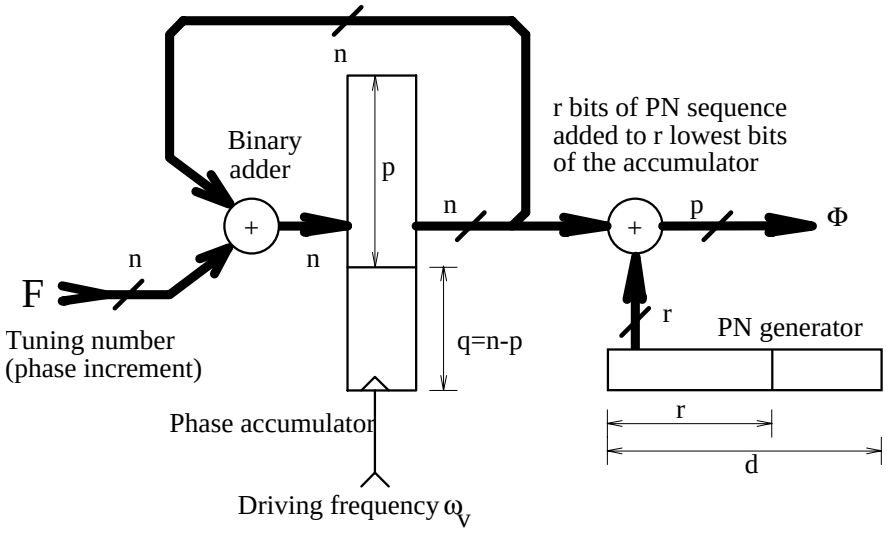

Figure 15: First order phase dithering architecture.

sequence binary generator with the generating primitive polynomial of degree d_p (d in Fig. 15) is used. Any part of the generator of the width r can be used for phase dithering. The M–sequence period is $R = 2^{d_p} - 1$ and this is also the period of the number sequence formed by taking any r output bits of the shift register forming the generator.

The simulation challenge lies in the fact that the number R is odd and for d_p prime it is also prime. The period of an non–dithered phase signal is m, given by (73), which is always a power of 2. Because the dithering sequence is periodic, the resulting signal is also periodic with the period given by

$$\mathrm{LCM}\,(m, R) = mR.$$

Even for small values of d_p the size of the period, and therefore the size of the discrete Fourier transform for determining the signal spectrum, is huge. The noise floor level is lower for longer periods of the dithering sequence.

What remains to be determined is the value of the dither "width" r. If the dither width $r < q$, then we can expect that the dither will not work too well, because in many cases its influence would remain burried in the truncated part of the phase accumulator. If $r > q$, then we would always dither the desired part of the phase value and therefore we would increase noise floor without really contributing to the power spreading of the spurious signals. Therefore, the best choice of the dither width is

$$r = q. \tag{79}$$

This fact was confirmed by many simulations and yielded the best results.

The performance of the first–order dither method is demostrated in Fig. 16 and Fig. 17.

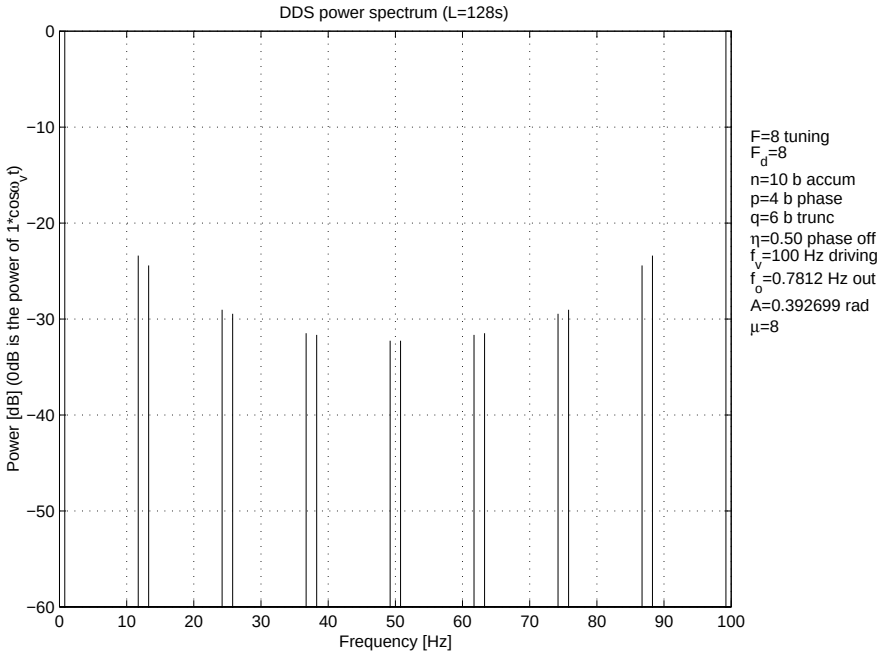

Figure 16: The spectrum without a phase dithering.

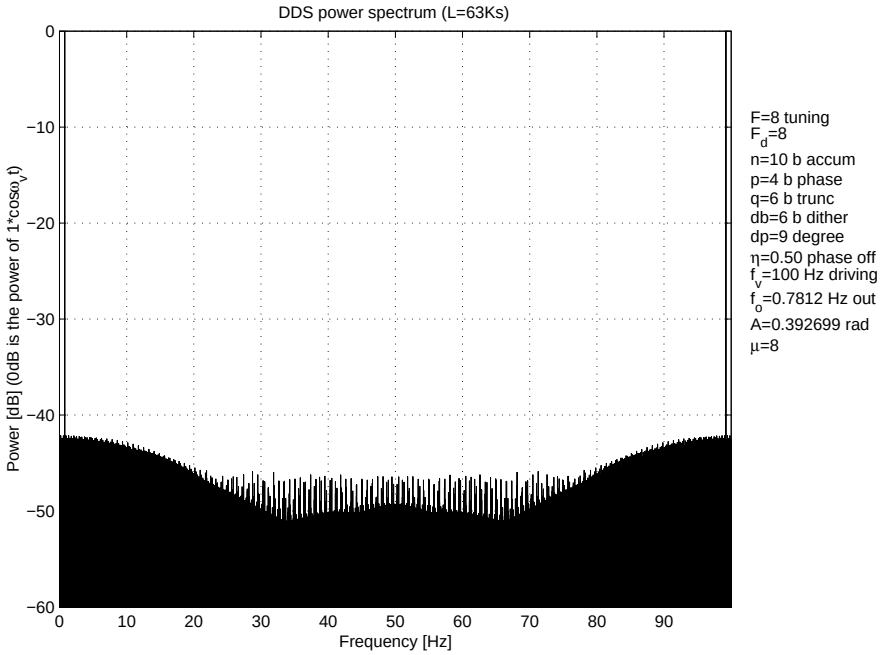

Figure 17: Spectrum of the phase–dithered signal.

6.2 Time domain representations

The folowing set of figures shows the signal representation in different stages of the DDS system. All figures were generated for $n = 11, p = 6, q = 5, b = 3, \mu = 4, d_b = 6$:

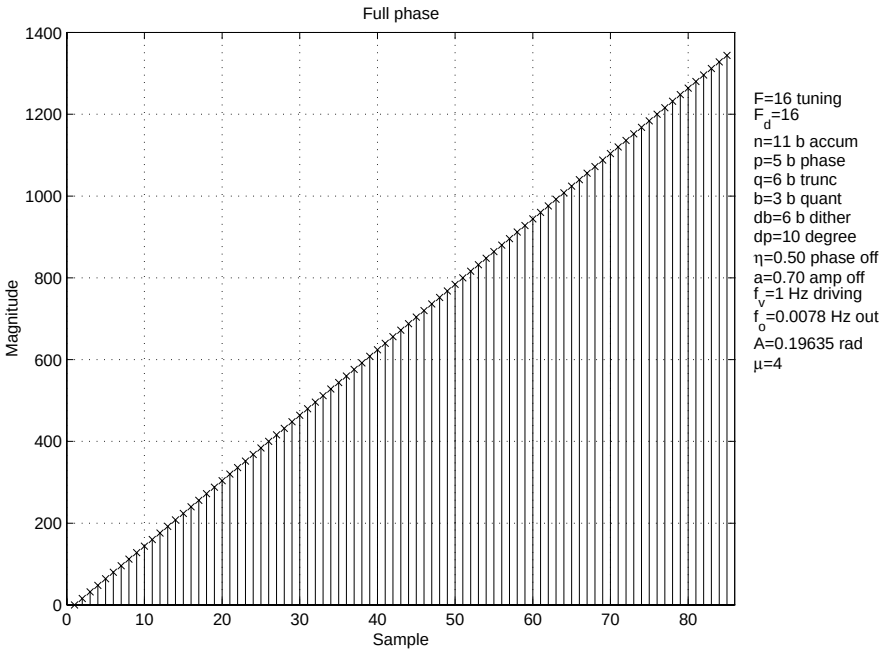

Figure 18: Generated linearly increasing phase (accumulator content).

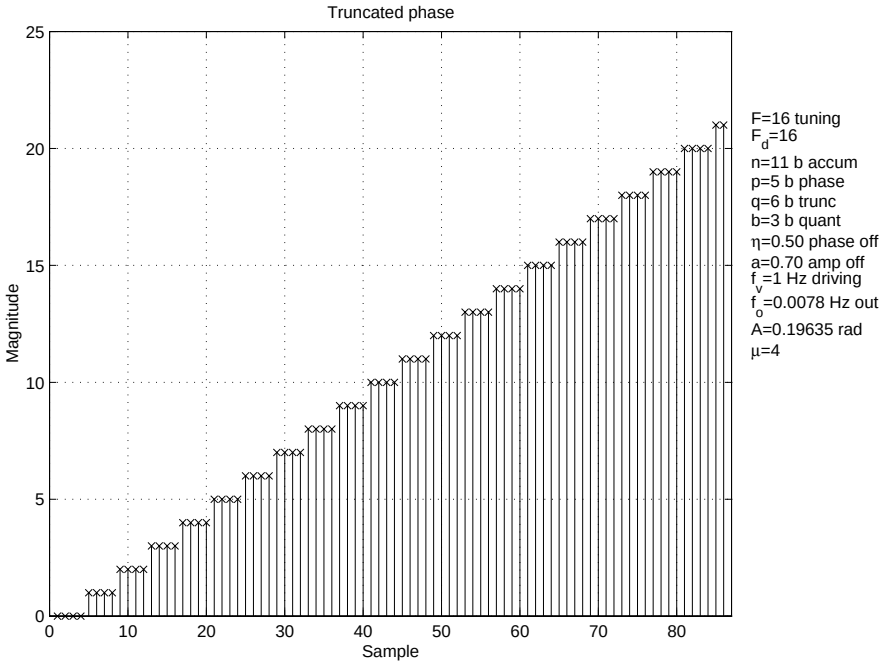

Figure 19: Truncated non-dithered phase.

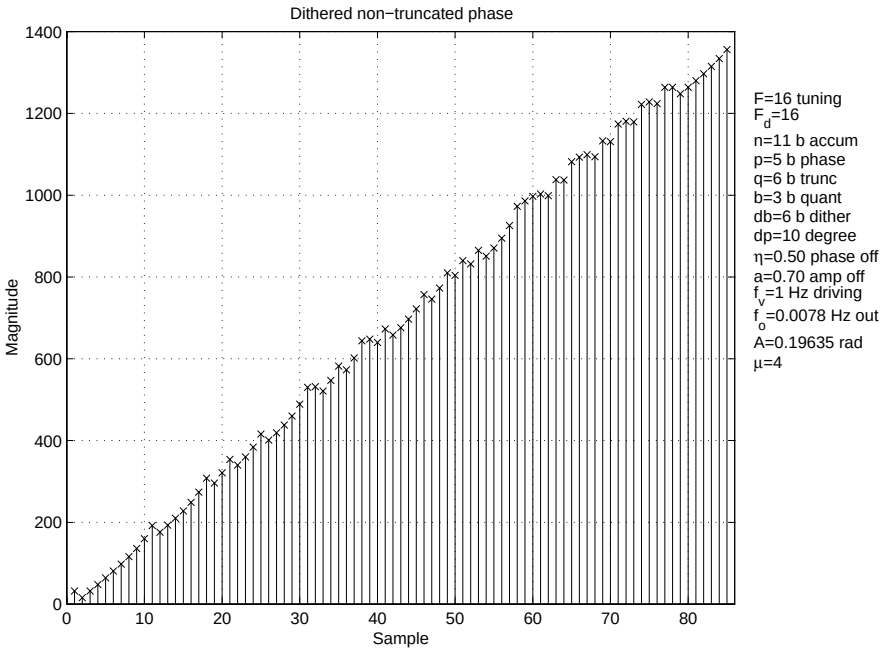

Figure 20: Dithered phase before accumulator phase truncation.

7 Conclusion

The output spectrum of DDS under the phase–truncation and amplitude–quantization has been calculated. The final expression for the phase–truncation spectrum has been improved over the one in [1]. The amplitude–

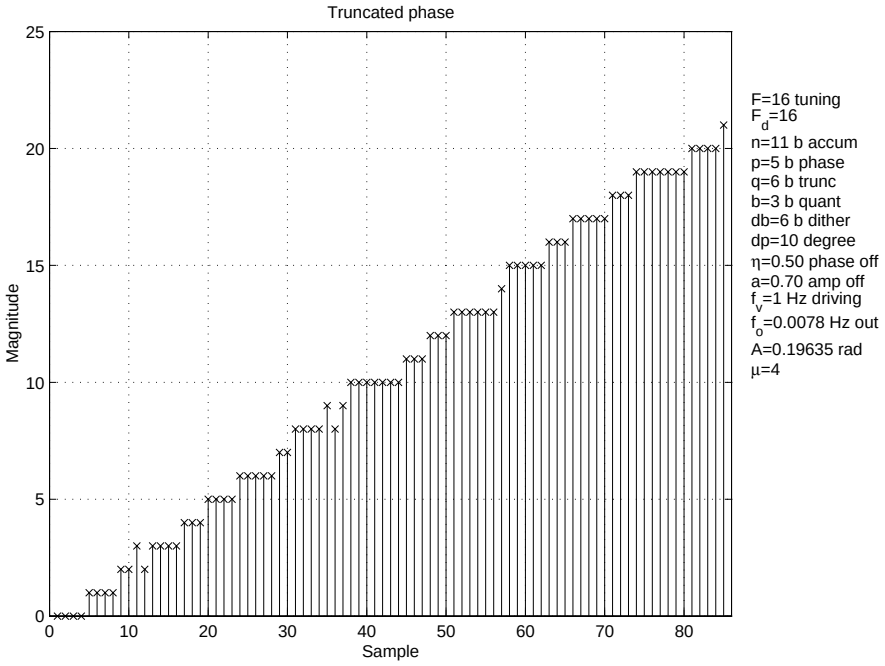

Figure 21: Truncated dithered phase.

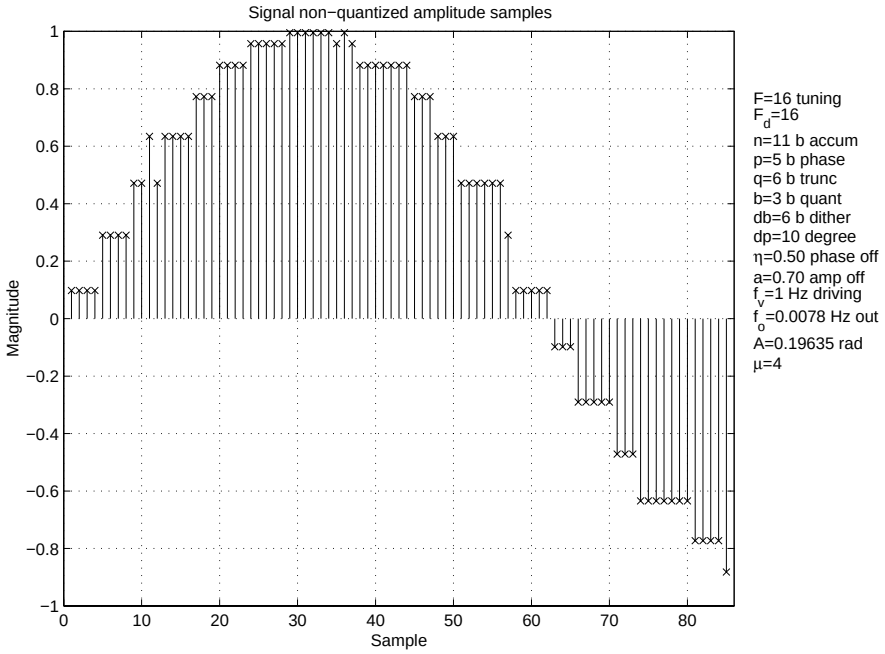

Figure 22: Signal amplitude before quantization.

quantization spectrum is an additive spectrum to the phase–truncation one. In the case when both the

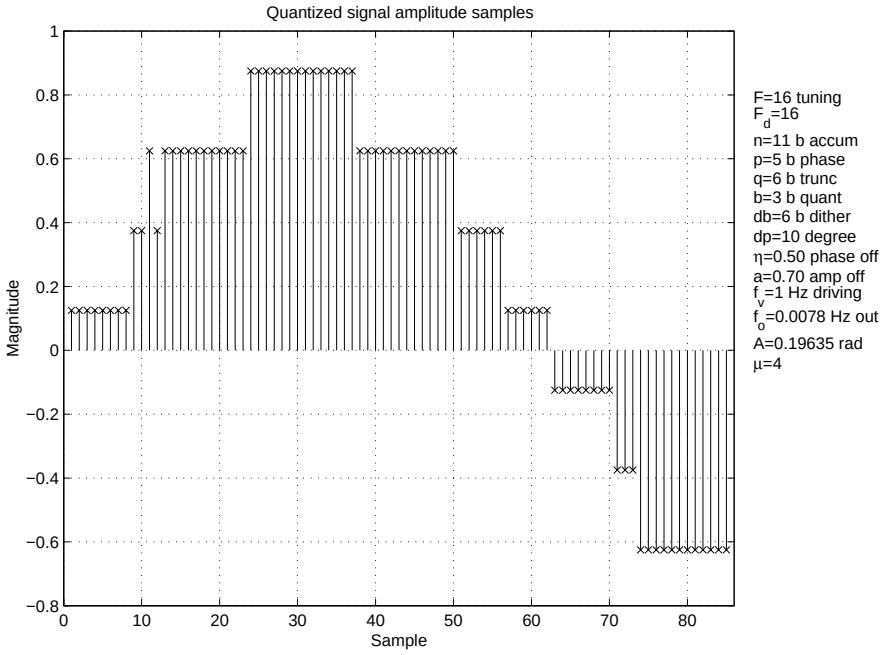

Figure 23: Signal quantized amplitude – output signal.

phase–truncation and amplitude–quantization are present, the output spectrum is the sum of the phase–truncation (no quantization) spectrum and the phase–modulated amplitude–quantization spectrum, which is minimal exactly at the spectral lines of the phase–quantization spectrum. The simulation enviroment with a graphic user interface was developed in MATLAB. The first–order phase dithering method was simulated and it was shown that it could be very effective in reducing the signal spurs caused by the phase–truncation.

References

[1] Henry T. Nicholas and Henry Samueli, "An analysis of the output spectrum of direct digital frequency synthetisers in the presence of phase–accumulator truncation," in *Proc. 41st Annual Frequency Control Symp.*, Ft. Monmouth, NJ, May 1987, USERACOM, pp. 495–502.

[2] J. Tierney, C. M. Rader, B. Gold, and J. Doe, "A digital frequency synthesizer," *IEEE Trans. Audio Electroacoust.*, vol. AU–19, pp. 48–57, 1971.

[3] Henry T. Nicholas, "The determination of the output spectrum of direct digital frequency syntersizers in the presence of phase accumulator truncation," M.S. thesis, UCLA, 1985.

[4] L. Jolley, *Summation of Series*, Chapman and Hall, London, 1925.

[5] Paul O´Leary and Franco Maloberti, "A direct–digital synthesiser with improved spectral performance," *IEEE Trans. Comm.*, vol. 39, no. 7, pp. 1046–1048, July 1991.

[6] Jouko Vankka, "Spur reduction techniques in sine output direct digital synthesis," in *Proc. 50st Annual Frequency Control Symp.*, 1996, pp. 951–959.

[7] M. J. Flanagan and G. A. Zimmerman, "Spur-reduced digital sinusoid synthesis," *IEEE Trans. Comm.*, vol. 43, no. 7, pp. 2254–2262, July 1995.

[8] M. J. Flanagan and G. A. Zimmerman, "Spur-reduced digital sinusoid generation using higher-order phase dithering," in *27th Annual Asilomar Conf. on Signals, Systems, and Computers*, Nov. 1993, pp. 826–830.

[9] Victor R. Reinhardt, "Spur reduction techniques in direct digital synthesizers," in *Proc. 47st Annual Frequency Control Symp.*, 1993, pp. 230–241.

[10] G. A. Zimmerman and M. J. Flanagan, "Spur-reduced numerically-controlled oscillator for digital receivers," in *26th Annual Asilomar Conf. on Signals, Systems, and Computers*, Dec. 1992, pp. 517–520.

[11] Jouko Vankka, "Methods of mapping from phase to sine amplitude in direct digital synthesis," in *Proc. 50st Annual Frequency Control Symp.*, 1996, pp. 942–950.

[12] Joseph F. Garvey and Daniel Babitch, "An exact spectral analysis of a number controlled oscillator based synthesizer," in *Proc. 44st Annual Frequency Control Symp.*, 1990, pp. 511–520.

[13] Henry T. Nicholas, Henry Samueli, and Bruce Kim, "The optimization of direct digital frequency synthetizer in the presence of finite word length effects," in *Proc. 42nd Annual Frequency Control Symp.*, 1988, pp. 357–363.